



Sediment organic carbon and temperature effects on methylmercury concentration: A mesocosm experiment

K.L. Buckman^{a,*}, E.A. Seelen^b, R.P. Mason^b, P. Balcom^{b,c}, V.F. Taylor^d, J.E. Ward^b, C.Y. Chen^a

^a Department of Biological Sciences, Dartmouth College, Hanover, NH, United States of America

^b Department of Marine Science, University of Connecticut, Groton, CT, United States of America

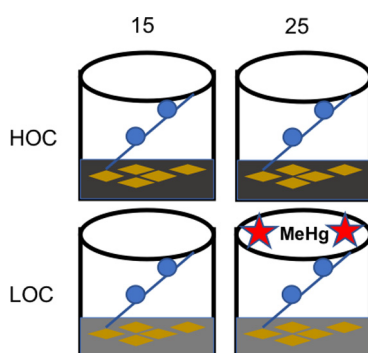
^c Harvard John A. Paulson School of Engineering and Applied Sciences, Cambridge, MA, United States of America

^d Department of Earth Science, Dartmouth College, Hanover, NH, United States of America

HIGHLIGHTS

- Climate change is predicted to influence carbon loading and temperature in estuaries.
- Estuaries are important areas for methylmercury production and bioaccumulation.
- Mesocosms examined effect of temperature and sediment organic carbon on MeHg.
- Water column MeHg, not sediment concentration, related to biota MeHg
- Sediment carbon influenced MeHg bioaccumulation more than temperature

GRAPHICAL ABSTRACT



ARTICLE INFO

Article history:

Received 30 October 2018

Received in revised form 1 February 2019

Accepted 19 February 2019

Available online 20 February 2019

Guest Editor: J. Rinklebe

Keywords:

Methylmercury
Bioaccumulation
Mesocosm
Invertebrate
Organic carbon
Temperature

ABSTRACT

The fate and mobility of mercury, and its bioaccumulation primarily as methylmercury (MeHg), in marine ecosystems are influenced by climate related environmental factors, including increased temperature and carbon loading. To investigate the interactions between sediment organic carbon and temperature MeHg bioaccumulation, mesocosm experiments were conducted examining relationships between sediment, water column and biota (sediment-dwelling amphipod and juvenile oyster) MeHg concentration. Experimental treatments consisted of a two by two design of high and low temperature (15 & 25 °C) and high and low sediment organic carbon (4–5% and 13% LOI, pre-experiment). Sediment organic carbon had significant individual effects on MeHg concentration in water and biota, with higher carbon associated with lower MeHg. Temperature individual effects were significant for sediment, water, and only amphipod MeHg concentration, with higher temperature treatments indicating higher MeHg concentration. There were significant temperature × carbon interactions observed for sediment, dissolved, and oyster MeHg concentration. Sediment carbon reduction had greater influence than temperature on increasing MeHg concentrations in both the water column and biota. MeHg concentrations in the bulk sediment were not correlated with MeHg in the water column or in the biota, indicating that even when sediments are the only source of MeHg, bulk sediment measurements do not provide a good proxy for bioaccumulation and that the concentration in bulk sediments is not the primary determinant of MeHg entry into the food web.

© 2019 Elsevier B.V. All rights reserved.

* Corresponding author at: Dept. of Biological Sciences, Dartmouth College, 78 College St. – LSC 6044, Hanover, NH 03755, United States of America.

E-mail address: Kate.L.Buckman@dartmouth.edu (K.L. Buckman).

1. Introduction

Mercury (Hg) cycling in the biosphere has been directly altered by human activity, and its fate and transformations in air, land, and water are indirectly influenced by local and global anthropogenic factors (Hsu-Kim et al., 2018; Obrist et al., 2018). Methylmercury (MeHg), the most bioavailable form of Hg, is bioaccumulated and biomagnified in aquatic food webs and the main exposure route for humans and wildlife is through the consumption of fish, with many people consuming mostly coastal species (Driscoll et al., 2013; Eagles-Smith et al., 2018; Sunderland, 2006). Reducing inputs of Hg to the environment has been the focus of recent international efforts to control global sources through the recently ratified Minamata Convention which aims to protect human health and the environment from anthropogenic emissions and releases of mercury throughout its life cycle (Chen et al., 2018; UNEP, 2013). While controlling Hg release is critical, as inputs are a major factor influencing the relative amount of MeHg that ends up in the human food chain, many other factors alter the net formation, bioavailability, and uptake of MeHg, resulting in a non-linear relationship between Hg loading and MeHg in the food chain. Our current understanding of mercury cycling and transformation suggests that the most important drivers of mercury transformation and bioaccumulation are not just the sources to the environment but other global alterations, such as climate change, and the presence of legacy contamination, especially in coastal environments (Obrist et al., 2018; Selin et al., 2018). Alterations to marine environments due to climate change are both direct through impacts on hydrologic cycles, water temperature, and ocean circulation, but also interact with other anthropogenic influenced processes such as nutrient loading and the resulting changes in the productivity and carbon flux from sediments and other reservoirs (Doney et al., 2012). These alterations in both the sediment and water column have the potential to influence the net production and bioavailability of MeHg within aquatic ecosystems.

Among the most important factors related to climate alteration in coastal ecosystems are increases in temperature and precipitation, particularly for temperate regions such as the Northeast US. The Gulf of Maine, for example, is undergoing rapid increases in temperature and has had the greatest increase in temperature over the last 50 years of any marine ecosystem in the world (Pershing et al., 2015). Increased temperatures should enhance the methylation of inorganic Hg (iHg) in the coastal environment as well as increase metabolic rates and MeHg bioaccumulation into estuarine fauna (Carrie et al., 2010; Driscoll et al., 2013; Marvin-DiPasquale and Agee, 2003). While increased temperatures are associated with increases in uptake of metals, including MeHg, into the base of the food chain, there is not an equivalent increase in elimination with temperature, which should result in relatively increased body burdens (Dijkstra et al., 2013; Sokolova and Lannig, 2008).

In addition, precipitation amount and storm intensity in the Northeast US are predicted to increase on the order of 50% in the next 30 years (USGCRP, 2017), which will enhance nutrient, watershed organic carbon (OC), Hg and MeHg transport to coastal ecosystems (Balch et al., 2016; Pinkney et al., 2015). Climate induced increases in precipitation can indirectly increase organic carbon loading to sediments (Driscoll et al., 2012), which will change Hg fate and burial in coastal sediments, and therefore sediment-water exchange of Hg and MeHg (Hollweg et al., 2010). Higher water column productivity can lead to increased methylation (Bravo et al., 2017) and under certain conditions, higher relative concentration of MeHg in phytoplankton (Soerensen et al., 2016). More commonly, eutrophication can also lead to biomass dilution of MeHg in the water column resulting in lower relative bioaccumulation of MeHg in primary consumers (Chen and Folt, 2005; Driscoll et al., 2012; Pickhardt et al., 2002; Soerensen et al., 2016). However, decreased concentration in primary consumers with eutrophication is not always found, or predicted by modeling, given the impact of eutrophication on zooplankton bioenergetics (Schartup

et al., 2018). Higher dissolved organic carbon (DOC) inputs, which could occur with higher productivity and through higher watershed inputs, have been found to cause trophic shifts at the base of the food web leading to higher MeHg accumulation (Jonsson et al., 2017). However, in contrast, laboratory culture experiments and phytoplankton uptake models (Luengen et al., 2012; Schartup et al., 2018) provide evidence that increased DOC will decrease bioaccumulation into phytoplankton, in conjunction with changes in phytoplankton size and composition. Alternatively, terrestrially sourced organic carbon from watersheds can flood and settle out in estuaries resulting in increased sequestration of Hg (Soerensen et al., 2017). At the same time, increased carbon loading to the sediment can also result in increased anoxia, and increased methylation rates under some conditions (Schartup et al., 2013b), while there is also evidence for higher sediment methylation in lower organic content sediments (Hammerschmidt and Fitzgerald, 2004; Hollweg et al., 2009). Overall, however, increased sediment organic carbon typically results in a lower flux of dissolved MeHg from sediments to the water column (Hollweg et al., 2010; Mason et al., 2006). In summary, climate change is predicted to have varied and at times contrasting effects on transport, sequestration, transformation, and bioaccumulation of Hg and MeHg in sediments and biota, yet these combined effects have been little studied for estuarine environments.

Past studies suggest that MeHg concentrations in sediment do not directly drive MeHg concentrations in water, particulates and biota (Balcom et al., 2015; Chen et al., 2014) primarily because of the importance of sediment characteristics in controlling sediment-water exchange of MeHg (Hollweg et al., 2010; Seelen et al., 2018). This disconnect results in Hg transformation processes and MeHg concentrations in bulk sediment not being predictive of MeHg bioaccumulation and trophic transfer in pelagic species. Given the disconnect between the bulk sediment Hg and MeHg concentrations and the water column concentrations, the impacts of temperature and sediment organic carbon on MeHg cycling may also be separated into sediment and bioaccumulation compartments. Since sediments are the largest repository of Hg in estuarine ecosystems but bioaccumulation is largely from the water column, it is important to understand the degree to which temperature and sediment organic carbon have individual and interactive effects on sediment vs. water column processes, and enhance or hinder the transfer of MeHg between these two reservoirs. Moreover, the combined effects of temperature and sediment organic carbon between and within compartments may be synergistic or antagonistic, which would influence the net impacts on MeHg production, flux, and bioaccumulation. These outcomes need to be considered in evaluating the effectiveness of global controls on Hg at local scales in light of climate change predictions.

In this study, we designed a mesocosm experiment to investigate the individual and combined impacts of temperature and sediment organic carbon on water column MeHg and its bioaccumulation into invertebrates. With our study design, we addressed the following questions regarding MeHg fate in estuaries: 1) Do temperature and sediment MeHg to organic carbon ratios (MeHg:TOC) have individual and interactive effects on sediment and water column MeHg concentration? 2) Do temperature and sediment MeHg:TOC have individual and interactive effects on MeHg concentration in benthic and pelagic primary consumers? and 3) Does MeHg concentration in primary consumers relate to MeHg concentration in sediments and/or the water column? We used a two by two factor experimental design in estuarine mesocosms to address these questions in order to determine the individual and combined effects of these climate change associated factors on MeHg fate. Additionally, we developed bioaccumulation models to validate that the differences found among treatments in terms of MeHg concentrations in biota were reasonable given our knowledge on how DOC, temperature and sediment carbon content influence MeHg fate and transport and the bioaccumulation process. We also used the models to assess the factors influencing uptake of MeHg into primary producers and the primary invertebrate consumers under the conditions in these experiments.

2. Methods

Bioaccumulation experiments with amphipods (*Leptocheirus plumulosus*) and juvenile oysters (*Crassostrea virginica*) were conducted at two temperatures (15 & 25 °C) and two sediment organic matter concentrations (unaltered sediments-HOC, sediment diluted with sand-LOC). Each organic carbon level-temperature treatment (LOC-15, LOC-25, HOC-15, HOC-25) consisted of 5 replicate exposure chambers (17 L volume) with animals, and 3 control chambers without animals.

2.1. Experimental chambers

For the experimental treatments, sediments collected from the Thames River (CT) during June 2014 were sieved (825 µm) to remove macro-organisms and debris, and portions stored at each test temperature. The HOC treatments were unaltered sediment (13% loss-on-ignition, LOI, pre-experiment). A portion of the sediment was diluted with sieved/rinsed playground sand to generate LOC sediment (target 4–5% LOI, pre-experiment). Sediment was distributed to exposure chambers to provide a sediment depth of 5 cm. Inorganic mercury (1.5 mL of 1000 ppm HgCl₂ per chamber) and methylmercury (2.1 mL of 1 ppm MeHgCl per chamber) were added to the LOC sediments so that the starting mercury concentrations were approximately the same in the HOC and LOC treatments. Sand and Hg addition methods were adapted from Lawrence and Mason (Lawrence and Mason, 2001). After sediment addition, the exposure chambers were filled with 100 µm filtered seawater from Long Island Sound that had been diluted to 24 ppt using deionized water, and the sediment-water combination was allowed to equilibrate for one week in temperature-controlled walk-in experimental chambers.

After the equilibration week, water was sampled from several test chambers, a partial (~20%) water change was completed on all chambers, and animals were added. Four juvenile oysters (1 cm in shell height), glued to glass rods, and 60 amphipods were added to each experimental chamber at time 0 (t_0). The green alga, *Tetraselmis* sp., chosen due to its ease of growth and wide use as bivalve food, was added to all chambers at t_0 and at weekly intervals when water was changed. At t_0 an extra chamber from each treatment was sacrificed to collect initial sediment samples.

Mesocosm chambers were arranged on vertical shelving in the environmental chambers, and treatments were interspersed in relation to shelf height and lighting (side-mounted next to chambers) and were supplied with aeration (Supporting Information (SI), Fig. S1). Approximately 20% water changes (100 µm filtered seawater adjusted to 24 ppt) occurred weekly after water was sampled from each exposure chamber. Temperature, salinity and dissolved oxygen (DO) were monitored before and several days after water changes, and temperature and salinity adjustments were made as necessary. Evaporation was minimized by covering chambers with plastic bags. The DO in the upper 4 cm of sediment was monitored in separate experimental cores over 4 days to examine the rate of sediment equilibration after mixing. DO profiles changed from oxic to anoxic within a few hours of sediment addition, and oxygen penetration in all treatments was low (<10% of water concentrations at 0.5 cm depth in all treatments). The final average DO profiles are presented in SI Fig. S2.

2.2. Sediment spiking

The LOC sediments were spiked with Hg and MeHg to achieve equal concentrations of Hg species between treatments. Sediment was allowed to equilibrate for 1 week as preliminary experiments suggested that less than 4 days was required for establishment of stable redox conditions in both LOC and HOC sediments (Fig. S2). In addition, work in freshwater sediment slurries had suggested that spiked iHg equilibrated to the solid phase in hours to days (Hintelmann and Harris, 2004) and that the half-life of spiked MeHg was less than 2 days (Hintelmann

et al., 2000). This prior work led us to believe that any initial increase in bioavailability or methylation due to “new” Hg being added would have stabilized by the end of the week, and the spiked Hg would behave similarly to the “native” Hg. In addition, the weekly trends in concentration, and the variability over time in the LOC tanks versus the HOC tanks, were carefully examined to ensure that the dynamics in the LOC mesocosms were not impacted by the spiked Hg and MeHg behaving differently than the ambient Hg in terms of transformation or bioavailability. Overall, there were no dramatic changes in water column concentration over time in either the spiked (LOC) or unspiked (HOC) mesocosms (Fig. S4); and there was not an observed early spike release to the water column in LOC tanks (as evaluated by week 0 vs weeks 1–4 dissolved concentration). This suggests a rapid sediment-water equilibrium that persisted throughout the experiment, and therefore similar mobility between the sediment and overlying water in spiked and unspiked sediment treatments. The similarity in sediment and water % MeHg between HOC and LOC treatments further suggests that the added spikes reached similar bioavailability to background Hg pools.

Most of the spiked Hg and MeHg remained in the sediment with <1% of the total Hg and MeHg being in the dissolved plus particulate in the water column throughout the experiments. Additionally, the spiked amount of Hg was environmentally relevant as the ratios of Hg to sediment organic matter were in the range of coastal estuarine sediments (range for the molar ratio of Hg to carbon, log Hg/C –5.0 to –7.5; (Schartup et al., 2013b)) for both the LOC sediments (log Hg/C ~ –5.3) and the HOC sediments (log Hg/C ~ –6.1); The %MeHg in the sediment (LOC: 0.15–0.34%, HOC: 0.06–0.32%) and water column (part. LOC: 0.22–0.79% HOC: 0.09–0.87%) were also within the range found in the environment, and the water column %MeHg and logK_d's were similar for the LOC and HOC treatments. These comparisons convince us that the LOC spiked mesocosms had realistic concentrations and distribution of Hg and MeHg relative to carbon, and between sediments and water, and that there was no artifact associated with spiking the LOC mesocosms.

2.3. Sample collection and analysis

At weeks 0, 1, 2, and 4 aqueous samples were collected from each chamber and filtered onto pre-combusted QFF filters. Filtered water samples were analyzed for total mercury (THg), MeHg, DOC, and nutrients. Particulate samples were frozen for later analysis of THg, MeHg, total suspended solids (TSS), and chl *a*. After 4 weeks, the experiments were terminated, water was sampled, grab samples of the top few cm of sediment were taken, and biota were collected. Amphipods surviving in test chambers were separated from sediment by sieving (825 µm) and oyster rods removed and cleaned of any accumulated algal growth. Both amphipods and oysters were frozen for later analysis.

Sediment and water analyses were conducted at the University of Connecticut Department of Marine Sciences. Sediment %LOI was determined by combustion at 550 °C for 8–12 h. Sediments were freeze dried and THg was analyzed using a Nippon DMA pyrolytic analyzer. The average (SE) relative percent difference (RPD) was 10% (2%) for sediment analytical duplicates, and average reference material recoveries were 113% (1%) for NRCC PACS-2. THg in dissolved and particulate (digested using 4 N HNO₃) water fractions were measured using purge and trap (dual gold-amalgamation) cold vapor atomic fluorescence spectrometry (Tekran 2500 CVAFS detector) (Balcom et al., 2015; Bloom and Fitzgerald, 1988; Bloom and Creclius, 1983; Fitzgerald and Gill, 1979). The average (SE) RPD for preparation and analytical duplicates were 5% (1%) and 8% (2%), respectively, for water and particulate samples. Aqueous HgT standard recoveries averaged 104% (2%). Sample results were corrected for field and preparation blanks as appropriate.

MeHg in filtered water, the particulate fraction, and sediment was analyzed after derivatization (ethylation) using purge and trap (Tenax) CVAFS (Tekran 2700 methylmercury analyzer). Water and sediment samples were distilled (Hammerschmidt and Fitzgerald, 2001;

Tseng et al., 2004) and particulate samples were acid leached with 2 N HNO₃ (Hammerschmidt and Fitzgerald, 2001). The average (SE) RPD for preparation and analytical duplicates were 14 (3) and 9 (2), respectively, for water and particulate samples. MeHg standard spiked sample and aqueous standard recoveries averaged (SE) 115% (4%) and 103% (2%), respectively, for water and particulate samples. Sediment MeHg average (SE) spiked sample and aqueous MeHg standard recoveries were 98% (14%) and 93% (2%), respectively. The average (SE) relative percent difference (RPD) for sediment MeHg analytical duplicates were 4% (1%). Sample results were corrected for field and preparation blanks as appropriate.

Biotic samples were analyzed for MeHg and inorganic Hg (iHg) tissue concentrations at the Dartmouth Trace Element Analysis Core by species-specific isotope dilution using an automated MeHg system MERX-M (Brooks Rand Labs, Seattle, WA) interfaced with an Element 2 ICP-MS (Thermo, Bremen, Germany), in an adaptation of EPA method 1630 (Taylor et al., 2011; Taylor et al., 2008). Total mercury was calculated as the sum of MeHg and iHg concentrations. Percent recovery for MeHg in certified reference values were 103 ± 9% for NIST 2976 Mussel (National Institute of Standards and Technology), 115% for NIST 1566B Oyster (National Institute of Standards and Technology), and 102% for DORM-4 (National Research Council of Canada). Recoveries for total Hg were 120 ± 22% for NIST 2976 Mussel, 97% for NIST 1566B, and 107% for DORM-4.

2.4. Data analysis

Two-way ANOVA was used to compare the four OC-temperature treatments for abiotic (dissolved aqueous, particulate, and sediment) MeHg concentrations, DOC, and biotic MeHg (amphipod and oyster) concentrations using JMP Pro13 (SAS). Data were log-transformed prior to analysis. The design was balanced and therefore robust to violations of assumptions for all analyses except oyster MeHg, as one LOC 15 °C treatment was found to contain empty oyster shells upon harvesting. Analyses tested for OC, temperature, and temperature x OC interactions using a standard least squares approach. To determine the relationship between abiotic variables chosen *a priori* to be relevant to possible routes of exposure and biotic MeHg concentrations, the Spearman's Rank Correlation test was used. Non-parametric test was chosen for this analysis as it is more conservative. For water column concentrations, a simple average of weeks 0, 1, 2 and 4 concentration was performed and used in the correlations. The time series data are provided in the Supporting Information (SI). For individual mesocosms where there was no week 0 measurement, the treatment average of the mesocosms analyzed for that week was substituted. Control (no animal) data are provided in the SI. Differences between MeHg concentration in experimental versus control treatments were examined using *t*-test within each treatment.

2.4.1. Bioaccumulation modeling

Modeling of biotic tissue concentrations was employed to validate that the measured concentrations were realistic based on knowledge of the factors controlling bioaccumulation, and to evaluate the relative importance of the pathway of MeHg exposure to the oysters and amphipods. The main source of MeHg to the water column was assumed to be from the sediment as a dissolved species, with dissolved MeHg concentrated by the phytoplankton which was subsequently consumed by the biota, as suggested by the correlation analysis. Alternatively, sediment bound MeHg could be consumed directly by the amphipods or resuspended by their burrowing activity for uptake by the oysters. If the latter situation prevailed, the models based on water column concentrations would not accurately predict our measured concentrations.

1) *Phytoplankton uptake*: The concentration of MeHg in the phytoplankton (C_{pp}) from uptake in the mesocosms was modeled based on Schartup et al. (2018), who modeled accumulation as related to

phytoplankton size which varied with chl *a* concentration. The MeHg uptake rate was modeled as dependent on the DOC and dissolved MeHg concentrations in the mesocosm and the surface area/volume (S/V) ratio of the phytoplankton size classes. For each fraction,

$$C_{pp} \text{ (ng/g wet weight)} = U \cdot C_w \cdot V/M$$

where C_w is the dissolved MeHg concentration (ng/L), V is the cell volume (μm^3), M is the wet weight (density $\times V$) and U is the uptake rate ($U = t \cdot (0.118S/V)e^{-0.008DOC}$), and it is assumed that plankton reach steady state concentrations after 4 h of exposure (so $t = 4$). The uptake rate equation was based on the literature (Lee and Fisher, 2016; Luengen et al., 2012) and it was assumed that uptake is not influenced by temperature (Schartup et al., 2018). The S/V used was 0.53 for *Tetraselmis*. Additional details are outlined in the SI.

2) *Assimilation into amphipods*: As amphipods were only collected at the end of the experiment, the model approach for uptake was fashioned after Williams et al. (2010), who estimated the steady state concentrations. The relevant equation for amphipods (C_{AM}), including uptake from water and from food, is:

$$C_{AM} = \frac{k_u \cdot C_w}{k_{ew} + G} + \frac{IR \cdot AE \cdot C_{pp}}{k_{ef} + G}$$

where k_u is the uptake rate constant from water ($1.6 \text{ L g body mass}^{-1} \text{ d}^{-1}$) and k_{ew} is the elimination rate of MeHg assimilated from water ($3 \times 10^{-5} \text{ d}^{-1}$), G the growth rate ($0.04\text{--}0.1 \text{ d}^{-1}$), and k_{ef} is the elimination rate constant for MeHg assimilated from food (0.052 d^{-1} ; (Williams et al., 2010)). The uptake from food is determined by the ingestion rate (IR ; $\text{g food g}^{-1} \text{ d}^{-1}$), the assimilation efficiency (AE ; 0.8; (Williams et al., 2010)) and the concentration in the food (C_{pp}). The IR values were based on particulate MeHg levels in each tank, assuming this as the dominant food source. The IR is affected by temperature (as is G and the other bioenergetics parameters). Therefore the model was run using two different IR scenarios, and with different values for the other bioenergetic variables, for each temperature. More details on the parameters and the model are included in the SI.

3) *Assimilation into oysters*: As the oysters did not grow appreciably during the experiment (growth rate $\sim 0.001 \text{ d}^{-1}$ based on dry mass of tissue at beginning and end), the steady state model used for amphipods could not be applied. The uptake into the oysters over time was modeled using the typical bioaccumulation model approach of relating concentration (C_o) to the rate of uptake and elimination of MeHg, and assuming no uptake directly from water:

$$C_o = \frac{k_1}{k_2} \cdot C_{pp}(1 - \exp(-k_2 \cdot t))$$

where k_1 is the uptake rate constant, which was derived using literature values for the filtration rate of oysters with temperature ($1.6 \text{ L g}^{-1} \text{ dry mass hr}^{-1}$ at 15 °C; $6.48 \text{ L g}^{-1} \text{ h}^{-1}$ at 25 °C; (Newell et al., 2005)), the measured TSS and particulate MeHg concentrations and the initial oyster concentrations. Here, k_2 is the loss rate constant, which is a combination of k_{ef} and G ($k_2 = k_{ef} + G$). From the measured oyster tissue dry masses at the beginning and end of the experiments, an average growth rate (G) of 0.001 d^{-1} was estimated, or a $\sim 3\%$ increase over the duration of the experiment. Reported values for k_{ef} of 0.003 d^{-1} for the oyster *Saccostrea cucullata* feeding on diatoms (Pan and Wang, 2011) were used along with G to estimate a value of k_2 of 0.005 d^{-1} at 15 °C, with a 10% increase for 25 °C.

3. Results

Both individual and interactive effects of sediment carbon and temperature treatments on MeHg concentration were observed, but the larger influence in both biotic and abiotic compartments was related to sediment OC manipulation, which yielded differing MeHg:OC ratios between HOC and LOC sediments.

3.1. Abiotic carbon \times temperature effects

3.1.1. Sediment MeHg

For experimental mesocosm chambers, ANOVA analysis indicated significant differences in sediment MeHg concentration between treatments (whole model: $R^2 = 0.76$, $F_{3,16} = 16.94$, $p < 0.0001$). There was no individual carbon effect ($p = 0.07$), which was the intended outcome of the sediment spiking, but there was an individual temperature effect ($p < 0.0001$). On average, sediment MeHg concentration in the LOC treatment did not differ between temperature treatments, but at HOC there was a significant temperature effect with lower temperature resulting in lower MeHg (Fig. 1a). The MeHg in the low temperature HOC was significantly lower than all other treatments. As a result, there was a significant temperature-carbon interaction ($p = 0.0039$). For %MeHg in sediment (Fig. 1b), there was no effect of temperature within carbon treatments, but at 15 °C, %MeHg was higher in LOC. There was no difference between LOC and HOC treatments at high temperature (whole model: $R^2 = 0.55$, $F_{3,16} = 6.47$, $p = 0.0045$). Sediment MeHg concentration differed between experimental (with animals) and control (no animals) mesocosms only for the 15 °C LOC treatment (SI Table S1).

3.1.2. Aqueous MeHg

ANOVA analysis indicated significant effects for particulate MeHg (whole model: $R^2 = 0.93$, $F_{3,16} = 73.14$, $p < 0.0001$) and dissolved MeHg (whole model: $R^2 = 0.97$, $F_{3,16} = 191.93$, $p < 0.0001$). LOC treatments had higher average dissolved and particulate MeHg concentrations (Fig. 2a & b). There was a small but significant temperature carbon interaction in dissolved concentrations ($p = 0.03$) resulting in statistically higher dissolved MeHg in higher temperature treatments

only in the HOC mesocosms (Fig. 2a). Experimental chambers had higher dissolved MeHg concentration than control chambers for the 15 and 25 °C LOC treatments and higher particulate MeHg concentration in the experimental chamber for the 15 °C HOC treatment only (Table S1).

Overall, the phytoplankton uptake model was able to predict particulate concentrations (Fig. S5). While the original Schartup model calculates the phytoplankton size based on the chl *a* concentration, we modeled the uptake assuming the particles were dominated by accumulation into *Tetraselmis* as this was added to the mesocosms throughout the experiment, and was likely the dominant large phytoplankton algae in the tanks. Size analysis, based on Coulter Counter data, confirmed that the majority of the suspended material was within the size range consistent with *Tetraselmis*. Across treatments with different temperatures and sediment organic content, and those with or without added organisms (amphipods, oysters), the relationship between the measured and modeled concentrations in the seston were similar except for some of the 25 °C HOC tanks where the model underpredicted the concentration (Fig. S5). Given the similarities in DOC between the treatments which strongly impacts MeHg uptake (Luengen et al., 2012; Schartup et al., 2018), the main variable controlling phytoplankton concentration in the mesocosms, and in the model, was the dissolved MeHg concentration which differed mostly between the LOC and HOC treatments. According to Schartup et al. (2018), temperature has little impact on the uptake rate and therefore on phytoplankton concentrations.

3.1.3. Dissolved organic carbon

Average DOC concentrations were calculated across weeks 1, 2 and 4 with one outlier removed from week 1 in the 25 °C HOC treatment. Significant differences in average DOC concentration were indicated by ANOVA analysis (whole model: $R^2 = 0.80$, $F_{3,16} = 21.77$, $p < 0.0001$). Higher temperature resulted in higher DOC across carbon treatments ($p < 0.0001$). Surprisingly, within temperature treatments, there was no significant difference in water column DOC between sediment organic carbon treatments ($p = 0.85$, Fig. 2c). Filamentous algal growth was observed on oyster rods in high T, high OC chambers.

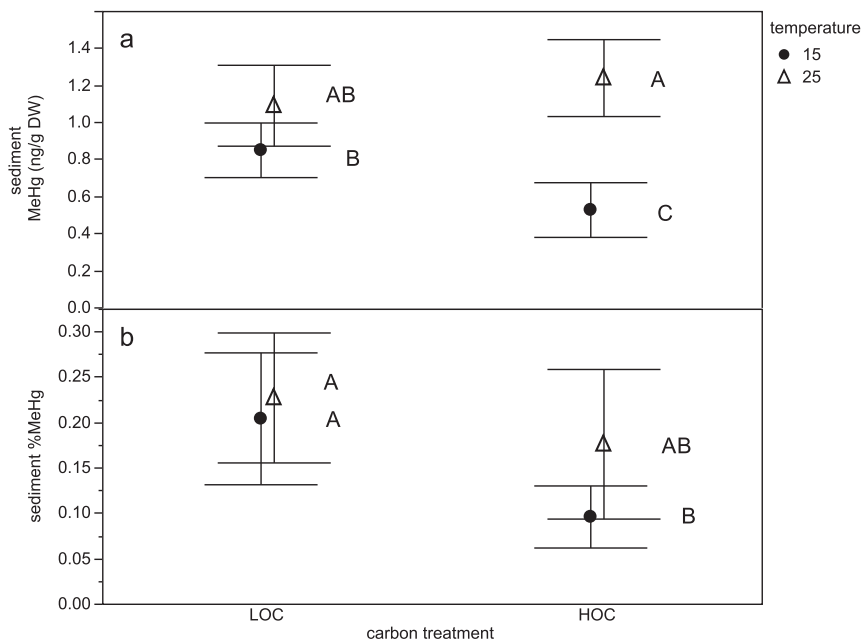


Fig. 1. sediment MeHg (a) and %MeHg (b) mean \pm st. dev. across temperature and sediment carbon (HOC–natural sediment, LOC–sand addition) treatments. Different letters indicate significant differences as assessed by Tukey's HSD.

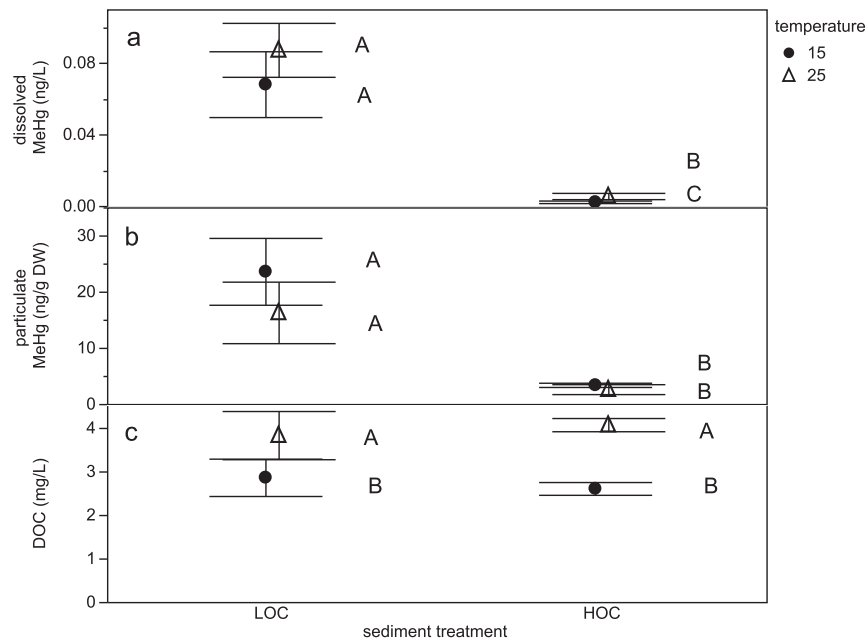


Fig. 2. Water MeHg (dissolved, upper panel; particulate, middle panel) and DOC (lower panel) concentrations. Mean and st. dev. across temperature and sediment (HOC-unmanipulated; LOC-sand addition) treatments. LOC sediment treatments represent a higher MeHg:OC ratio than HOC treatments.

3.2. Biotic carbon \times temperature effects

3.2.1. Amphipod bioaccumulation

ANOVA analysis indicated significant differences among all treatments for MeHg concentration of the sediment-dwelling amphipod (whole model: $R^2 = 0.98$, $F_{3,16} = 278.88$, $p < 0.0001$). Higher temperature resulted in greater tissue concentration of MeHg ($p = 0.0002$) and lowered sediment organic carbon also resulted in a higher MeHg concentration ($p < 0.0001$), but there was not a significant interaction effect between temperature and sediment carbon ($p = 0.77$) (Fig. 3a). The temperature effect on amphipod tissue concentration in the HOC treatments was quite small (6.7 ± 1.2 ng/g at 15 °C versus 10.3 ± 1.5 ng/g at 25 °C), but was statistically significant. Tissue concentrations in

amphipods were best predicted by the bioaccumulation model that utilized measured phytoplankton concentrations and included an increased temperature effect on ingestion rate and the other bioenergetics parameters (Fig. S6), as would be expected (Williams et al., 2010).

To demonstrate and contrast the various potential impacts of climate change, a sensitivity analysis was done using the amphipod and phytoplankton models and the potential changes in water column variables associated with climate change. Using the 15 °C LOC tanks as an example, the model predicts that a 1 °C (7%) increase would lead to a 18% increase in amphipod concentration, which is somewhat larger than found in the experiments, where a 10 °C increase in temperature lead to an approximate doubling in the concentration in amphipods. Alternatively, for DOC, a 20% increase in DOC for these tanks would lead to

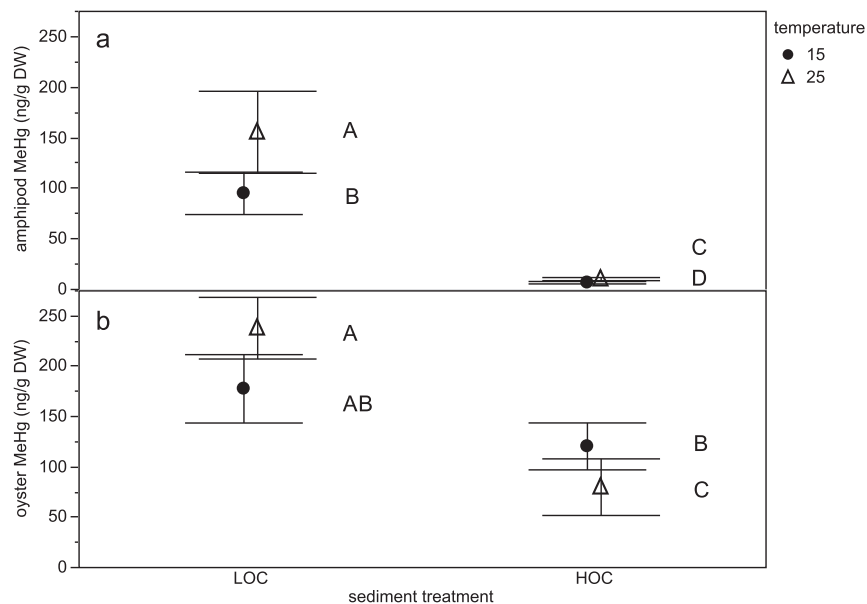


Fig. 3. Effect of sediment treatment (HOC-unmanipulated; LOC-sand addition) and temperature on MeHg bioaccumulation. Amphipod (a) and oyster concentration (b) mean and st. dev. of MeHg concentration on a dry weight basis.

a 21% decrease in amphipod concentration. These calculations assume no change in sediment organic content or water column MeHg.

3.2.2. Oyster bioaccumulation

Similar to amphipods, there were significant differences in MeHg concentration among treatments for oysters ($R^2 = 0.80$, $F_{3,15} = 20.02$, $p < 0.0001$) (Fig. 3). There was no temperature effect ($p = 0.53$), but there was a significant sediment treatment effect ($p < 0.0001$) with greater concentration in LOC treatments, and a significant temperature \times sediment carbon interaction ($p = 0.0047$) resulting in an increase in MeHg concentration at 15 °C for the HOC treatment only. Modeled bioaccumulation was in good agreement with measured tissue concentrations for oysters (Fig. S7).

3.3. Relationship of biotic MeHg to abiotic parameters

Spearman's rank correlation analysis indicated that MeHg tissue concentration in both amphipods and oysters was not related to sediment MeHg concentration but was related to both dissolved and particulate MeHg concentration (Fig. 4, Table 1). Moreover, biotic MeHg concentrations were not significantly correlated with TSS, DOC or chl a , all variables that have been predicted to have a potential effect on bioaccumulation. In addition, sediment MeHg concentration was not correlated with either particulate ($\rho = -0.13$ $p = 0.59$) or dissolved ($\rho = 0.35$ $p = 0.14$) MeHg concentrations for the experimental chambers.

4. Discussion

Changes in climate are likely to cause shifts in sediment organic carbon loading and temperature within estuarine systems. These environmental shifts may have significant, but competing effects on MeHg production and bioaccumulation. With documented increases in seawater temperature in the Gulf of Maine and predicted increases in precipitation in the Northeast US (Pershing et al., 2015; USGCRP, 2017), the relative degree of change in each of these variables will in part

Table 1

Relationship of biotic MeHg concentrations to abiotic MeHg and ancillary factors across all treatments combined. One DOC outlier was excluded from analysis (week 1, HOC, 25 °C treatment). One particulate MeHg outlier (week 4, LOC-4) was also excluded.

Biotic MeHg	Abiotic	Spearman's ρ (p)
Oyster	Sediment MeHg	−0.06 (0.81)
	Particulate MeHg	0.69 (<0.01)
	Dissolved aqueous MeHg	0.67 (<0.01)
	TSS	0.14 (0.57)
	DOC	−0.14 (0.58)
	Chlorophyll a	0.14 (0.56)
Amphipod	Sediment MeHg	0.39 (0.09)
	Particulate MeHg	0.61 (<0.01)
	Dissolved aqueous MeHg	0.90 (<0.01)
	TSS	0.14 (0.56)
	DOC	0.28 (0.24)
	Chlorophyll a	0.34 (0.15)

determine whether MeHg production and/or bioavailability increases or decreases. If increased organic carbon loading in estuaries (both sediment and watershed OC, assuming similar Hg loading) has a stronger influence than increased temperature, these interactions are predicted to result in decreased MeHg bioaccumulation at the base of coastal food webs which will decrease the trophic transfer of MeHg to fish that humans consume (e.g. (Driscoll et al., 2012)). Conversely, should changes in sea level, precipitation, development, or productivity result in decreased OC delivery to coastal sediments, a relative increase in methylation and/or bioaccumulation could result due to enhanced sediment or water column net methylation.

4.1. Impact of sediment organic carbon on overlying water

In our mesocosm experiment manipulating sediment to achieve lower levels of sediment organic carbon (higher MeHg:TOC) resulted in higher concentrations of MeHg in the water column, and subsequently higher concentrations in the biota. The role of organic matter is complex in mediating Hg methylation and the percentage of Hg

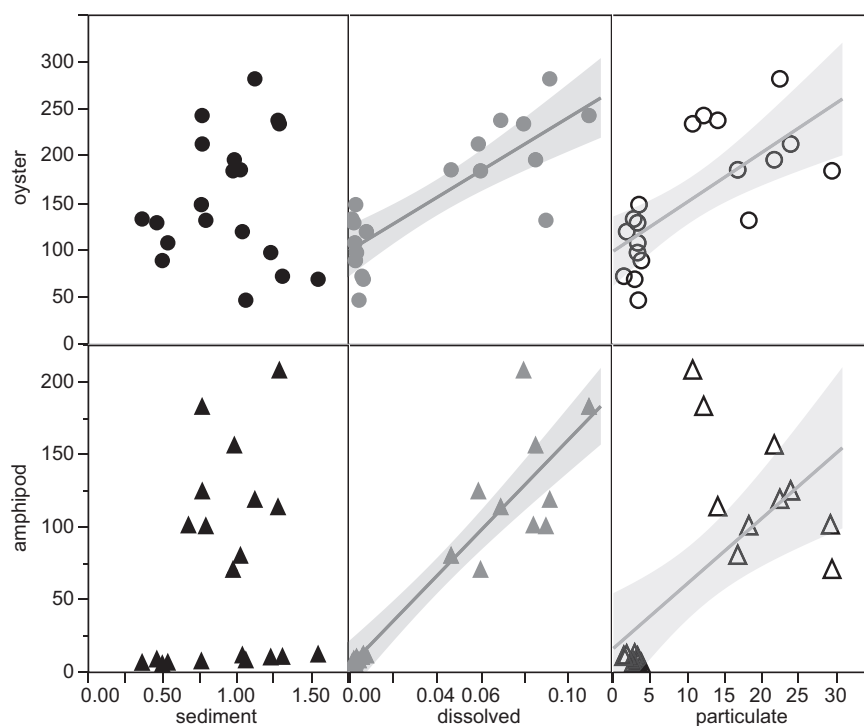


Fig. 4. Scatterplot relationships of sediment (black), dissolved water (grey), and particulate (open) MeHg concentration to amphipod (triangle) and oyster (circle) MeHg concentration. Significant correlations are indicated by best fit lines and 95% confidence intervals (shaded).

present in sediments as MeHg (Liu et al., 2015), as well as MeHg flux from sediments and bioavailability. While high sediment organic carbon has been associated with increased mercury methylation rates and higher MeHg concentrations in sediments (Lambertsson and Nilsson, 2006; Schartup et al., 2013a), this is not always the case (Hammerschmidt and Fitzgerald, 2004; Hammerschmidt et al., 2008; Hollweg et al., 2009). Furthermore, it is likely that other abiotic factors such as the sulfur chemistry and porewater sulfide concentration are better predictors of methylation and MeHg concentration in sediment than the bulk organic carbon content. Sediment chemistry has been proposed as the major control over MeHg flux from sediment to the overlying water (Hollweg et al., 2009; Hollweg et al., 2010; Mason et al., 2006), along with oxygen content of overlying water and redox conditions of the sediment (Gill et al., 1999). In addition, methylation rates have been suggested to exert some control over flux as well (Mason et al., 2006). In the current study, similar %MeHg, which is often used as a proxy for methylation rates, did not differ between sediment carbon treatments, particularly at the higher temperature, despite predictions that higher Hg relative to carbon (e.g. the LOC treatments) would lead to greater methylation than in the unmanipulated low Hg:TOC sediments (Schartup et al., 2013b). Percent MeHg was relatively low overall (~0.2%) and similar to field samples at six of 11 sites found in Schartup et al. (Schartup et al., 2013b) spanning a range of %LOI (0.7–11%) also similar to our experimental sediment carbon content. In addition, the overlying water was well oxygenated (>80%) and sediment oxygen profiles were similar across treatments (Fig. S2), leading us to believe that differences in redox conditions did not strongly influence flux. Sediment OC has also been shown to increase partitioning to the solid phase, making mercury less bioavailable for methylation and for MeHg to flux to overlying water, (Hammerschmidt et al., 2008), and this is likely the major difference controlling the MeHg flux differences between treatments and dominating MeHg dynamics within the current mesocosm system, as evidenced by the low water column MeHg concentrations in the HOC treatments relative to LOC.

To further examine this, we estimated porewater concentrations and flux of MeHg using the relationship between $\log K_D$ for MeHg and sediment OC in Hammerschmidt et al. (Hammerschmidt et al., 2004), data on porewater sulfide and MeHg speciation from Hollweg et al. (Hollweg et al., 2009; Hollweg et al., 2010) for sediments from that study with similar OC to the HOC and LOC sediments, and the method of estimating MeHg flux based on porewater and overlying water MeHg speciation in Hollweg et al. (Hollweg et al., 2010). These calculations suggest that the diffusive flux of MeHg from the LOC sediments was about 10 times higher than for the HOC sediments. These flux differences are driven mostly by the large difference in predicted porewater MeHg for the HOC sediments (estimated as 0.4–1.1 pM for the different treatments) compared to the LOC sediments (6.7–13.9 pM). Overall, the flux difference between HOC and LOC treatments are of the same order as the differences in dissolved water column MeHg concentrations (Fig. 2). Since there were weekly water changes from the same source water, the differences between treatments in water column variables are driven by the influence of the sediment characteristics on the MeHg flux, and the resultant impact on the water column MeHg within each week. The data suggest that there was a greater flux of MeHg from the sediments to the water column in the LOC tanks, which is consistent with the calculations above and other sediment diffusive flux studies (Gagnon et al., 1996; Gill et al., 1999; Hammerschmidt et al., 2008; Hollweg et al., 2010; Mason et al., 2006). We hypothesize that under sediment conditions of similar Hg and MeHg concentrations, similar methylation rates, similar redox conditions, similar sediment grain size, and similar carbon composition/quality, that MeHg:TOC within the sediment is the main factor controlling the MeHg flux to the overlying water.

DOC has also been implicated in controlling MeHg persistence in the water column (Soerensen et al., 2017), and its bioavailability and

bioaccumulation (Schartup et al., 2015a; Schartup et al., 2018) where increasing DOC increases water column MeHg concentrations, but limits phytoplankton uptake of MeHg (Lee and Fisher, 2016; Schartup et al., 2018). Additionally, DOC source may also affect MeHg fate, with terrestrially derived DOC potentially inhibiting uptake into primary producers in marine systems more than marine-derived DOC (Schartup et al., 2015b) but also enhancing bioaccumulation near-shore (Jonsson et al., 2017). In the mesocosm experiments, there was a disconnect between the sediment carbon content and the DOC as while there was a substantial difference in %LOI between the HOC and LOC treatments, a DOC difference was not apparent. The lack of difference in DOC concentration between sediment carbon treatments suggests that the source of DOC was from water column biogeochemical cycling derived from algae and the input from sediments was small, with the observed temperature effect related to temperature-induced changes on growth, decay, and predation of the phytoplankton. Similar DOC concentrations across sediment carbon treatments suggests that in the mesocosm, DOC had a minimal influence on MeHg bioavailability and provides increased support for the hypothesis that sediment OC and chemistry was driving differences in flux of MeHg to the water column. Many studies have suggested a strong role for sediment OC and/or sulfur in binding MeHg in sediments and reducing its bioavailability and flux and the findings from the mesocosm studies provide further support for these hypotheses (Hammerschmidt et al., 2008; Hollweg et al., 2010; Lambertsson and Nilsson, 2006).

4.2. Drivers of bioaccumulation

The results of the mesocosm experiment also demonstrate that MeHg bioaccumulation into primary consumers was driven by water column MeHg and not related to sediment MeHg concentration. While this has been shown by correlation in field studies (Chen et al., 2014; Taylor et al., 2019), sediments were likely the only source of MeHg in this experimental system, whereas watershed sources may also contribute under field conditions. Overall, the extent of the sediment impact on bioaccumulation is a function of flux which is primarily controlled by both methylation rates and the sediment chemistry, particularly its organic matter content and composition. The lack of correlation between the water column and sediment MeHg in this experiment, and in various field studies, indicates the important control that sediment chemistry plays on the exchange of MeHg between sediment and water, as shown by field studies of MeHg fluxes from sediments (e.g. (Hollweg et al., 2010)). The cycling from the sediment to the water column ultimately determines the MeHg content of the resident biota, even for benthic organisms such as amphipods, rather than direct exposure to the sediment itself.

Higher levels of organic carbon in sediment were associated with lower concentrations of MeHg in both primary consumers. This correlates with the concentrations in dissolved and particulate MeHg in Fig. 2a&b. For amphipods, which feed on surface sediment detritus and more likely, settling and water column algae (Lawrence and Mason, 2001; Taylor et al., 2012), there were both significant OC effects and temperature effects. Tissue concentration was higher in LOC than HOC treatments and at higher temperature vs. lower temperature treatments, though the temperature effect was smaller in the HOC exposures (Fig. 3a), and was likely related to the impact of temperature on the organism's bioenergetics, as indicated by the modeling results discussed below. The increased concentration at LOC and high temperature is consistent with the water column dissolved MeHg differences, further supporting the role of the water column in driving bioaccumulation for these organisms. It is notable that an organism that resides in and has the opportunity to feed in the sediment is impacted by direct sediment exposure to the same degree as the completely pelagic oyster.

The lack of correlation between the bulk sediment MeHg and water column MeHg and/or biota MeHg has been interpreted to indicate that the role of sediments as a direct source of MeHg to the organisms is

minimal. It is also important to note that the bulk sediment measurements, typically a 0–2 cm sample, may not provide a representative measurement of the portion of the sediment interacting directly with the water column. Resuspension studies using estuarine sediments (Seelen et al., 2018) show that the MeHg content, and other characteristics, of the material being resuspended has little relationship to the bulk sediment MeHg, and tracks better with the suspended particulate MeHg, and that this material reflects a combination of sources, including settled material from the water column. This is also likely the layer that is the food source for the amphipods, which may explain why even in these organisms, their MeHg burden reflects the water column concentrations rather than that of the bulk sediment. Overall, the results of the mesocosm study are consistent with our field studies across northeastern estuaries (Balcom et al., 2015; Buckman et al., 2017; Chen et al., 2014; Taylor et al., 2019), in that sediment MeHg concentrations are not the best predictors of biota body burdens, which is relevant to assessments of contaminated sites and Hg remediation strategies.

4.3. Bioaccumulation models

To evaluate whether the experimental results are realistic, and to further examine the importance of water column processes and water column characteristics in driving bioaccumulation into the base of the food chain we modeled the MeHg concentration in the phytoplankton using the Schartup et al. (2018) bioaccumulation model, and the average measured values of dissolved MeHg and DOC for each mesocosm. In terms of the uptake of MeHg into the primary producers in the mesocosms, the model results confirm the conclusion that, given the similarity in DOC and the phytoplankton size distribution across the mesocosms, and the lack of a temperature effect, the dissolved MeHg was likely the main controlling variable determining seston concentrations. Overall, the model predicted phytoplankton concentrations for the LOC sediment mesocosms well, but overestimated their concentration in the HOC treatment. The modeling indicated that water column conditions mediate the amount of MeHg taken up into the base of the food web, and that this step is critical to consider for bioaccumulation. As the model was based on simplified uptake experiments without sediments, but was able to predict the phytoplankton MeHg concentrations in our experiments with sediments, the study provides further evidence that while the sediments influence the water column through flux of MeHg, there are also unique water column processes influencing uptake that are decoupled from the sediment.

The inaccurate prediction of seston MeHg concentrations in the HOC tanks was likely a consequence of the low MeHg concentrations found in these exposures, which would exacerbate any contribution of non-algal particulate to the overall measured concentration. The calculated C/Chl *a* ratio for the seston shows that while the ratio was typically <100 for the control tanks without animals, which is comparable to the range of values for phytoplankton (e.g. (Jakobsen and Markager, 2016)), the values were much higher in the tanks with animals (>100) suggesting that the seston contained substantial non-algal components, either due to sediment disturbance by amphipods, or due to the presence of fecal pellets and other particulate material derived from the animals present. This likely accounts for the underprediction of the model for these tanks.

Trophic transfer factors for amphipods (MeHg amphipod:MeHg particulate (i.e. their most likely food source) were about a factor of two higher at each temperature in the LOC tanks, and were also twice as high at 25 °C than at 15 °C for each treatment, suggesting that other factors besides the concentration in the food, such as metabolic rates, are important in determining amphipod concentrations (Table S2). Modeling the accumulation into amphipods using the constants in Williams et al. (2010) and the modeled seston concentrations in the current study lead to an underprediction of the amphipod MeHg concentration (Fig. S5), but the relative concentrations between treatments were as found in the experimental systems. However, increasing the IR rate

based on Arnot and Gobas (2004), which relates feeding rate to organism mass, and using the measured values of MeHg in seston resulted in predictions much closer to the measured amphipod MeHg values. The model results validate the notion derived from the correlation analysis, that the amphipod MeHg concentrations correlate best with dissolved and particulate MeHg, and are driven by pelagic processes, primary production, and metabolic rates, rather than by direct sediment exposure and ingestion. Additionally, using the information about the potential impact of temperature on IR, the differences in concentration found in this study appear reasonable.

Oysters, which are water column filter feeders, showed an increase in MeHg concentration for the LOC treatments, and at lower temperature for the HOC exposure. This contrasts with the results for the amphipods where there was an increase in MeHg bioaccumulation at higher temperature under both carbon conditions (Fig. 3). While this difference was surprising, increased growth of filamentous algae on the oyster rods was observed in the 25 °C HOC treatment and may have reduced their feeding efficiency and thus their bioaccumulation of MeHg. Modeling was used to further examine the factors controlling uptake into oysters from the suspended material. A steady state approach could not be used as the oysters did not grow appreciably during the experiment and the concentration in the oysters from the HOC 25 °C tanks (79.9 ± 28.1 ng/g MeHg DW) were even lower at the end of the experiment than the average value for the initial oysters (110 ± 21.5 ng/g MeHg), although the values are not statistically different. The model provided a good prediction of the concentrations in the LOC tanks at both temperatures and confirmed that the differences in the effect of temperature on IR, G and K_{ef} lead to a temperature effect such that the oysters in the higher temperature tanks had higher MeHg burdens, but not because of higher exposure concentrations. Based on knowledge of the effect of temperature on bioenergetics for bivalves, higher temperatures should result in higher concentrations because of the differences in the effect of temperature on filtration rate, assimilation efficiency, growth rate and depuration rate. The inability of the model to predict the concentration in the 25 °C HOC tanks is likely because of the impacts of biofouling on feeding in these tanks, as discussed above.

The model results generally aligned well with measured values (Fig. S8), and supported various notions about the effect of temperature and sediment carbon content on MeHg bioaccumulation into the pelagic and epipelagic food chain. Firstly, even in systems where the sediment is the dominant source of MeHg, the concentrations in the seston at the base of food chain are not directly related to the sediment characteristics but to the water column DOC, temperature, and dissolved MeHg concentration, with suspended solids content and food quality also impacting consumers. These water column metrics are only indirectly related to sediment characteristics. For primary consumers, the effect of temperature is measurable and is manifest because of its larger effect on MeHg uptake than on growth and depuration.

Sensitivity analysis of the amphipod and phytoplankton models show responsiveness to changes in temperature (increase T leads to increased amphipod MeHg) and DOC (increase leads to decrease in amphipod MeHg). The results of this study suggest that increases in sediment organic carbon concentration associated with climate change could decrease MeHg bioavailability and accumulation in estuarine food webs, but only if Hg and MeHg loading is not changed with increased watershed inputs of carbon. Realistically, increased precipitation and storm intensity will likely increase MeHg supply to coastal ecosystems due to enhanced transport of dissolved and particulate MeHg with organic matter into the coastal zone, which may confound the mitigating effects of relatively higher sediment carbon. A change in dissolved MeHg would lead to a similar directional change in biota concentration, all else being equal. Based on the mesocosm experiments, the differences in water column dissolved MeHg was a factor of 10–40 times higher in the LOC tanks while the %LOI was 8–10 times higher in the HOC tanks. These are large differences and given that the relationship

is non-linear, it is difficult to predict how smaller differences in sediment organic content would influence biota concentrations.

5. Conclusion

The combined experimental and modeling results indicate that even for estuarine systems where sediment is the dominant source of MeHg, the interactive effects of sediment biogeochemistry and temperature will overall determine sediment MeHg flux to the water column, and it is the resultant water column concentrations that determine the patterns of bioaccumulation in aquatic biota (Fig. 5). While sediment factors affecting methylation and flux are complex, under sediment conditions with relatively similar Hg loading, methylation rates, and redox conditions, the amount of OC in the sediment will be the dominant mediator of dissolved MeHg flux to the overlying water. Water column MeHg speciation, driven mostly by DOC concentration, and metabolic processes, which depend on temperature, will then drive bioaccumulation. The sediment carbon effect on bioavailability may interact with, but generally outweigh, the temperature influence on feeding and metabolism. However, the water column dynamics, in particular dissolved MeHg, DOC, and temperature will drive uptake into primary producers and consumers, and the subsequent bioaccumulation through the food web. The study supports the hypothesis that climate change impacts in coastal systems will likely cause substantial alterations in the bioaccumulation of MeHg into seafood consumed by humans, but that the effects will not always be synergistic and lead to higher bioaccumulation.

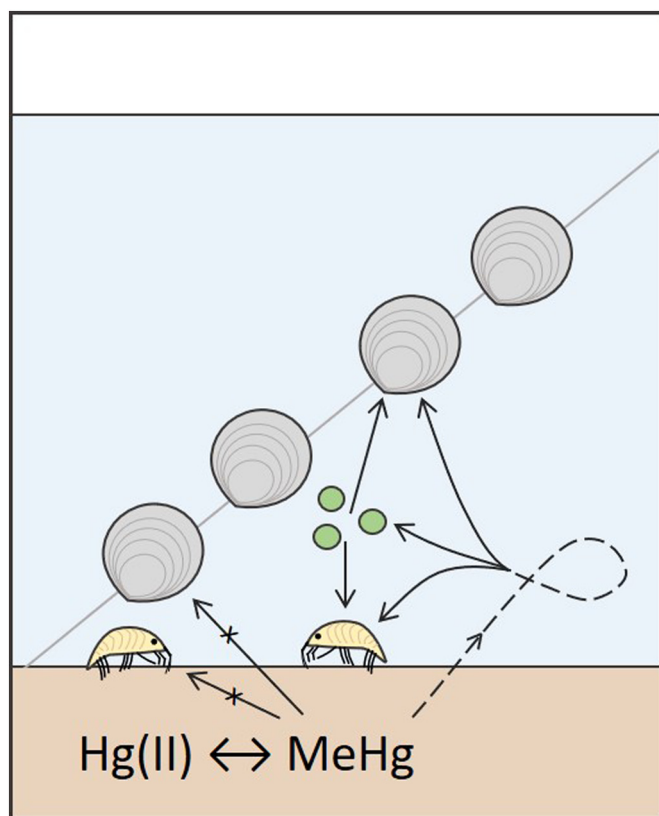


Fig. 5. Conceptual diagram of MeHg exposure and bioaccumulation into the mesocosm biota. Direct exposure from the sediment (solid line with “x”) is less important than flux to overlying water (dashed line), and water column exposure is mediated by uptake into primary producers (solid lines). The dashed line water column bioaccumulation is only indirectly related to sediment processes and characteristics, in particular MeHg:OC, which will impact flux to the overlying water under similar conditions of loading and methylation.

Acknowledgements

We wish to acknowledge B. Holohan and M. Zegans for assistance with mesocosm maintenance and take-down, and B. DiMento, K. Gosnell and V. Tanguay for mercury and ancillary parameter analyses. This work was supported by grants from the National Institute of Environmental Health Sciences, of the National Institute of Health under award numbers P42 ES007373 and R01ES021950. The contents of this manuscript are solely the responsibility of the authors and do not necessarily represent official views of NIEHS or NIH.

Appendix A. Supplementary data

Supplementary data to this article can be found online at <https://doi.org/10.1016/j.scitotenv.2019.02.302>.

References

- Arnot, J.A., Gobas, F., 2004. A food web bioaccumulation model for organic chemicals in aquatic ecosystems. *Environ. Toxicol. Chem.* 23, 2343–2355. <https://doi.org/10.1897/03-438>.
- Balch, W., Huntington, T., Aiken, G., Drapeau, D., Bowler, B., Lubelczyk, L., et al., 2016. Toward a quantitative and empirical dissolved organic carbon budget for the Gulf of Maine, a semienclosed shelf sea. *Glob. Biogeochem. Cycles* 30, 268–292. <https://doi.org/10.1002/2015gb005332>.
- Balcom, P.H., Schartup, A.T., Mason, R.P., Chen, C.Y., 2015. Sources of water column methylmercury across multiple estuaries in the Northeast US. *Mar. Chem.* 177, 721–730. <https://doi.org/10.1016/j.marchem.2015.10.012>.
- Bloom, N.S., Creclius, E.A., 1983. Determination of mercury in seawater at sub-nanogram per liter levels. *Mar. Chem.* 14, 49–59. [https://doi.org/10.1016/0304-4203\(83\)90069-5](https://doi.org/10.1016/0304-4203(83)90069-5).
- Bloom, N., Fitzgerald, W.F., 1988. Determination of volatile mercury species at the picogram level by low-temperature gas-chromatography with cold-vapor atomic fluorescence detection. *Anal. Chim. Acta* 208, 151–161. [https://doi.org/10.1016/S0003-2670\(00\)80743-6](https://doi.org/10.1016/S0003-2670(00)80743-6).
- Bravo, A.G., Bouchet, S., Tolu, J., Bjorn, E., Mateos-Rivera, A., Bertilsson, S., 2017. Molecular composition of organic matter controls methylmercury formation in boreal lakes. *Nat. Commun.* 8. <https://doi.org/10.1038/ncomms14255>.
- Buckman, K., Taylor, V., Broadley, H., Hocking, D., Balcom, P., Mason, R., et al., 2017. Methylmercury bioaccumulation in an urban estuary: Delaware River, USA. *Estuar. Coasts* 40, 1358–1370. <https://doi.org/10.1007/s12237-017-0232-3>.
- Carrie, J., Wang, F., Sanei, H., Macdonald, R.W., Outridge, P.M., Stern, G.A., 2010. Increasing contaminant burdens in an Arctic fish, Burbot (*Lota lota*), in a warming climate. *Environ. Sci. Technol.* 44, 316–322. <https://doi.org/10.1021/es902582y>.
- Chen, C.Y., Folt, C.L., 2005. High plankton densities reduce mercury biomagnification. *Environ. Sci. Technol.* 39, 115–121. <https://doi.org/10.1021/es0403007>.
- Chen, C.Y., Borsuk, M.E., Bugge, D.M., Hollweg, T., Balcom, P.H., Ward, D.M., et al., 2014. Benthic and pelagic pathways of methylmercury bioaccumulation in estuarine food webs of the Northeast United States. *PLoS One* 9. <https://doi.org/10.1371/journal.pone.0089305>.
- Chen, C.Y., Driscoll, C.T., Eagles-Smith, C.A., Eckley, C.S., Gay, D.A., Hsu-Kim, H., et al., 2018. A critical time for mercury science to inform global policy. *Environ. Sci. Technol.* 52, 9556–9561. <https://doi.org/10.1021/acs.est.8b02286>.
- Dijkstra, J.A., Buckman, K.L., Ward, D., Evans, D.W., Dionne, M., Chen, C.Y., 2013. Experimental and natural warming elevates mercury concentrations in estuarine fish. *PLoS One* 8. <https://doi.org/10.1371/journal.pone.0058401>.
- Doney, S.C., Ruckelshaus, M., Duffy, J.E., Barry, J.P., Chan, F., English, C.A., et al., 2012. Climate change impacts on marine ecosystems. In: Carlson, C.A., Giovannoni, S.J. (Eds.), *Annual Review of Marine Science*. vol 4(4), pp. 11–37.
- Driscoll, C.T., Chen, C.Y., Hammerschmidt, C.R., Mason, R.P., Gilmour, C.C., Sunderland, E.M., et al., 2012. Nutrient supply and mercury dynamics in marine ecosystems: a conceptual model. *Environ. Res.* 119, 118–131. <https://doi.org/10.1016/j.envres.2012.05.002>.
- Driscoll, C.T., Mason, R.P., Chan, H.M., Jacob, D.J., Pirrone, N., 2013. Mercury as a global pollutant: sources, pathways, and effects. *Environ. Sci. Technol.* 47, 4967–4983.
- Eagles-Smith, C.A., Silbergeld, E.K., Basu, N., Bustamante, P., Diaz-Barriga, F., Hopkins, W.A., et al., 2018. Modulators of mercury risk to wildlife and humans in the context of rapid global change. *Ambio* 47, 170–197.
- Fitzgerald, W.F., Gill, G.A., 1979. Sub-nanogram determination of mercury by 2-stage gold amalgamation and gas-phase detection applied to atmospheric analysis. *Anal. Chem.* 51, 1714–1720. <https://doi.org/10.1021/ac50047a030>.
- Gagnon, C., Pelletier, E., Mucci, A., Fitzgerald, W.F., 1996. Diagenetic behavior of methylmercury in organic-rich coastal sediments. *Limnol. Oceanogr.* 41, 428–434. <https://doi.org/10.4319/lo.1996.41.3.0428>.
- Gill, G.A., Bloom, N.S., Cappellino, S., Driscoll, C.T., Dobbs, C., McShea, L., et al., 1999. Sediment-water fluxes of mercury in Lavaca Bay, Texas. *Environ. Sci. Technol.* 33, 663–669. <https://doi.org/10.1021/es980380c>.
- Hammerschmidt, C.R., Fitzgerald, W.F., 2001. Formation of artifact methylmercury during extraction from a sediment reference material. *Anal. Chem.* 73, 5930–5936. <https://doi.org/10.1021/ac010721w>.

- Hammerschmidt, C.R., Fitzgerald, W.F., 2004. Geochemical controls on the production and distribution of methylmercury in near-shore marine sediments. *Environ. Sci. Technol.* 38, 1487–1495. <https://doi.org/10.1021/es034528q>.
- Hammerschmidt, C.R., Fitzgerald, W.F., Lamborg, C.H., Balcom, P.H., Visscher, P.T., 2004. Biogeochemistry of methylmercury in sediments of Long Island sound. *Mar. Chem.* 90, 31–52. <https://doi.org/10.1016/j.marchem.2004.02.024>.
- Hammerschmidt, C.R., Fitzgerald, W.F., Balcom, P.H., Visscher, P.T., 2008. Organic matter and sulfide inhibit methylmercury production in sediments of New York/New Jersey Harbor. *Mar. Chem.* 109, 165–182. <https://doi.org/10.1016/j.marchem.2008.01.007>.
- Hintelmann, H., Harris, R., 2004. Application of multiple stable mercury isotopes to determine the adsorption and desorption dynamics of Hg(II) and MeHg to sediments. *Mar. Chem.* 90, 165–173. <https://doi.org/10.1016/j.marchem.2004.03.015>.
- Hintelmann, H., Keppel-Jones, K., Evans, R.D., 2000. Constants of mercury methylation and demethylation rates in sediments and comparison of tracer and ambient mercury availability. *Environ. Toxicol. Chem.* 19, 2204–2211. [https://doi.org/10.1897/1551-5028\(2000\)019<2204:Commad-2.3.Co;2](https://doi.org/10.1897/1551-5028(2000)019<2204:Commad-2.3.Co;2).
- Hollweg, T.A., Gilmour, C.C., Mason, R.P., 2009. Methylmercury production in sediments of Chesapeake Bay and the mid-Atlantic continental margin. *Mar. Chem.* 114, 86–101. <https://doi.org/10.1016/j.marchem.2009.04.004>.
- Hollweg, T.A., Gilmour, C.C., Mason, R.P., 2010. Mercury and methylmercury cycling in sediments of the mid-Atlantic continental shelf and slope. *Limnol. Oceanogr.* 55, 2703–2722. <https://doi.org/10.4319/lo.2010.55.6.2703>.
- Hsu-Kim, H., Eckley, C.S., Acha, D., Feng, X.B., Gilmour, C.C., Jonsson, S., et al., 2018. Challenges and opportunities for managing aquatic mercury pollution in altered landscapes. *Ambio* 47, 141–169. <https://doi.org/10.1007/s13280-017-1006-7>.
- Jakobsen, H.H., Markager, S., 2016. Carbon-to-chlorophyll ratio for phytoplankton in temperate coastal waters: seasonal patterns and relationship to nutrients. *Limnol. Oceanogr.* 61, 1853–1868. <https://doi.org/10.1002/lno.10338>.
- Jonsson, S., Andersson, A., Nilsson, M.B., Skjellberg, U., Lundberg, E., Schaefer, J.K., et al., 2017. Terrestrial discharges mediate trophic shifts and enhance methylmercury accumulation in estuarine biota. *Sci. Adv.* 3. <https://doi.org/10.1126/sciadv.1601239>.
- Lambertsson, L., Nilsson, M., 2006. Organic material: the primary control on mercury methylation and ambient methyl mercury concentrations in estuarine sediments. *Environ. Sci. Technol.* 40, 1822–1829. <https://doi.org/10.1021/es051785h>.
- Lawrence, A.L., Mason, R.P., 2001. Factors controlling the bioaccumulation of mercury and methylmercury by the estuarine amphipod *Leptocheirus plumulosus*. *Environ. Pollut.* 111, 217–231. [https://doi.org/10.1016/s0269-7491\(00\)00072-5](https://doi.org/10.1016/s0269-7491(00)00072-5).
- Lee, C.S., Fisher, N.S., 2016. Methylmercury uptake by diverse marine phytoplankton. *Limnol. Oceanogr.* 61, 1626–1639. <https://doi.org/10.1002/lno.10318>.
- Liu, B., Schaidt, L.A., Mason, R.P., Shine, J.P., Rabalais, N.N., Senn, D.B., 2015. Controls on methylmercury accumulation in northern Gulf of Mexico sediments. *Estuar. Coast. Shelf Sci.* 159, 50–59. <https://doi.org/10.1016/j.ecss.2015.03.030>.
- Luengen, A.C., Fisher, N.S., Bergamaschi, B.A., 2012. Dissolved organic matter reduces algal accumulation of methylmercury. *Environ. Toxicol. Chem.* 31, 1712–1719. <https://doi.org/10.1002/etc.1885>.
- Marvin-DiPasquale, M., Agee, J.L., 2003. Microbial mercury cycling in sediments of the San Francisco Bay-Delta. *Estuaries* 26, 1517–1528.
- Mason, R.P., Kim, E.H., Cornwell, J., Heyes, D., 2006. An examination of the factors influencing the flux of mercury, methylmercury and other constituents from estuarine sediment. *Mar. Chem.* 102, 96–110. <https://doi.org/10.1016/j.marchem.2005.09.021>.
- Newell, R.I.E., Fisher, T.R., Holyoke, R.R., Cornwell, J.C., 2005. Influence of eastern oysters on nitrogen and phosphorus regeneration in Chesapeake Bay, USA. In: Dame, R.F., Olenin, S. (Eds.), *Comparative Roles of Suspension-Feeders in Ecosystems*. 47, pp. 93–120.
- Obrist, D., Kirk, J.L., Zhang, L., Sunderland, E.M., Jiskra, M., Selin, N.E., 2018. A review of global environmental mercury processes in response to human and natural perturbations: changes of emissions, climate, and land use. *Ambio* 47, 116–140. <https://doi.org/10.1007/s13280-017-1004-9>.
- Pan, K., Wang, W.X., 2011. Mercury accumulation in marine bivalves: influences of biodynamics and feeding niche. *Environ. Pollut.* 159, 2500–2506. <https://doi.org/10.1016/j.envpol.2011.06.029>.
- Pershing, A.J., Alexander, M.A., Hernandez, C.M., Kerr, L.A., Le Bris, A., Mills, K.E., et al., 2015. Slow adaptation in the face of rapid warming leads to collapse of the Gulf of Maine cod fishery. *Science* 350, 809–812.
- Pickhardt, P.C., Folt, C.L., Chen, C.Y., Klaue, B., Blum, J.D., 2002. Algal blooms reduce the uptake of toxic methylmercury in freshwater food webs. *Proc. Natl. Acad. Sci. U. S. A.* 99, 4419–4423. <https://doi.org/10.1073/pnas.072531099>.
- Pinkney, A.E., Driscoll, C.T., Evers, D.C., Hooper, M.J., Horan, J., Jones, J.W., et al., 2015. Interactive effects of climate change with nutrients, mercury, and freshwater acidification on key taxa in the North Atlantic landscape conservation cooperative region. *Integr. Environ. Assess. Manag.* 11, 355–369. <https://doi.org/10.1002/ieam.1612>.
- Schartup, A.T., Balcom, P., Chen, C., Mason, R.P., 2013a. An examination of the factors controlling net methylation in estuarine sediments: results from measurements and models. In: Pirrone, N. (Ed.), *Proceedings of the 16th International Conference on Heavy Metals in the Environment*. 1.
- Schartup, A.T., Mason, R.P., Balcom, P.H., Hollweg, T.A., Chen, C.Y., 2013b. Methylmercury production in estuarine sediments: role of organic matter. *Environ. Sci. Technol.* 47, 695–700. <https://doi.org/10.1021/es302566w>.
- Schartup, A.T., Balcom, P.H., Soerensen, A.L., Gosnell, K.J., Calder, R.S.D., Mason, R.P., et al., 2015a. Freshwater discharges drive high levels of methylmercury in Arctic marine biota. *Proc. Natl. Acad. Sci. U. S. A.* 112, 11789–11794. <https://doi.org/10.1073/pnas.1505541112>.
- Schartup, A.T., Ndu, U., Balcom, P.H., Mason, R.P., Sunderland, E.M., 2015b. Contrasting effects of marine and terrestrially derived dissolved organic matter on mercury speciation and bioavailability in seawater. *Environ. Sci. Technol.* 49, 5965–5972. <https://doi.org/10.1021/es506274x>.
- Schartup, A.T., Qureshi, A., Dassuncao, C., Thackray, C.P., Harding, G., Sunderland, E.M., 2018. A model for methylmercury uptake and trophic transfer by marine plankton. *Environ. Sci. Technol.* 52, 654–662. <https://doi.org/10.1021/acs.est.7b03821>.
- Seelen, E.A., Massey, G.M., Mason, R.P., 2018. Role of sediment resuspension on estuarine suspended particulate mercury dynamics. *Environ. Sci. Technol.* 52, 7736–7744. <https://doi.org/10.1021/acs.est.8b01920>.
- Selin, H., Keane, S.E., Wang, S., Selin, N.E., Davis, K., Bally, D., 2018. Linking science and policy to support the implementation of the Minamata convention on mercury. *Ambio* 47, 198–215.
- Soerensen, A.L., Schartup, A.T., Gustafsson, E., Gustafsson, B.G., Undeman, E., Bjorn, E., 2016. Eutrophication increases phytoplankton methylmercury concentrations in a Coastal Sea-a Baltic Sea case study. *Environ. Sci. Technol.* 50, 11787–11796. <https://doi.org/10.1021/acs.est.6b02717>.
- Soerensen, A.L., Schartup, A.T., Skrobonja, A., Bjorn, E., 2017. Organic matter drives high interannual variability in methylmercury concentrations in a subarctic coastal sea. *Environ. Pollut.* 229, 531–538. <https://doi.org/10.1016/j.envpol.2017.06.008>.
- Sokolova, I.M., Lannig, G., 2008. Interactive effects of metal pollution and temperature on metabolism in aquatic ectotherms: implications of global climate change. *Clim. Res.* 37, 181–201. <https://doi.org/10.3354/cr00764>.
- Sunderland, E.M., 2006. Mercury exposure from domestic and imported estuarine and marine fish in the US seafood market. *Environ. Health Perspect.* 115, 235–242.
- Taylor, V.F., Jackson, B.P., Chen, C.Y., 2008. Mercury speciation and total trace element determination of low-biomass biological samples. *Anal. Bioanal. Chem.* 392, 1283–1290. <https://doi.org/10.1007/s00216-008-2403-3>.
- Taylor, V.F., Carter, A., Davies, C., Jackson, B.P., 2011. Trace-level automated mercury speciation analysis. *Anal. Methods* 3, 1143–1148.
- Taylor, D.L., Linehan, J.C., Murray, D.W., Prell, W.L., 2012. Indicators of sediment and biotic mercury contamination in a southern New England estuary. *Mar. Pollut. Bull.* 64, 807–819. <https://doi.org/10.1016/j.marpolbul.2012.01.013>.
- Taylor, V., Buckman, K., Seelen, E., Mazrui, N., Balcom, P., Mason, R., et al., 2019. Organic carbon content drives methylmercury levels in the water column and in estuarine food webs across latitudes in the Northeast United States. *Environ. Pollut.* 246, 639–649.
- Tseng, C.M., Hammerschmidt, C.R., Fitzgerald, W.F., 2004. Determination of methylmercury in environmental matrices by on-line flow injection and atomic fluorescence spectrometry. *Anal. Chem.* 76, 7131–7136. <https://doi.org/10.1021/ac049118e>.
- UNEP, 2013. In: Branch, U.C. (Ed.), *Mercury: Acting Now!*, p. 24 Geneva Switzerland.
- USGCRP, 2017. *Climate science special report: fourth national climate assessment*. In: Wuebbles, D.J., Fahey, D.W., Hibbard, K.A., Dokken, D.J., Stewart, B.C., Maycock, T.K. (Eds.), *U.S. Global Change Research Program. Volume I*. Washington, DC, USA, p. 470.
- Williams, J.J., Dutton, J., Chen, C.Y., Fisher, N.S., 2010. Metal (As, Cd, Hg, and CH₃Hg) bioaccumulation from water and food by the benthic amphipod *Leptocheirus plumulosus*. *Environ. Toxicol. Chem.* 29, 1755–1761. <https://doi.org/10.1002/etc.207>.